A Simplified Hydrodynamic Impact Ionization Model Based on the Average Energy of Hot Electron Subpopulation

Ting-wei Tang and Joonwoo Nam
Dept. of Electrical & Computer Engineering
University of Massachusetts, Amherst, MA 01003 U.S.A.
e-mail: ttang@ecs.umass.edu fax:413-545-4611

Abstract - A simplified hydrodynamic model for impact ionization (II) is developed. The model is based on the average energy of hot electron subpopulation (HES) which is believed to be more relevant to the II than the average energy of total electron population (TEP). By solving this simplified HD model, II coefficient is calculated only as a function of the average energy of HES. The model is easily applicable to 2-D by exploiting the current flow line approach.

I. Introduction

In order for any hydrodynamic (HD) model to be useful as an engineering simulation tool, it should be easily implementable and produce reasonably accurate results within acceptable computation time. Although attempts have been made to construct a hot electron subpopulation (HES) HD model by taking the first few moments of the Boltzmann transport equation (BTE) [1],[2], application of the model to a realistic situation such as modeling of 2-D MOSFET devices encounters some difficulties. This comes primarily from inability to determine the correct boundary conditions for macroscopic variables because of scarcity of HES electrons at Ohmic contacts.

In this work, a further simplification of the previous works [1], [2] has been made to result in a HD equation consisting of the average energy of HES only. By solving this simplified HES HD equation, the II coefficient, α, is obtained only as a function of $w_2 = \langle\varepsilon\rangle_{\varepsilon\geq\varepsilon_{th}}$. For the application of the model to realistic MOSFET devices, the flow line approach [3] can be utilized to obtain 2-D profiles of α.

II. The HD Transport Equation for Hot Electron Subpopulation

The derivation of the simplified HES HD equation starts with the following three conservation equations for the HES electrons obtained from the BTE [1]:

$$\nabla\cdot\vec{j}_2 - \vec{F}\cdot\vec{\chi}_{n_2} = n_2 C_{n_2}, \tag{1}$$

$$\nabla\cdot(n_2\hat{U}_2) - n_2\vec{F} - \vec{F}\cdot\hat{\chi}_{p_2} = n_2\vec{C}_{p_2}, \tag{2}$$

$$\nabla\cdot(n_2\vec{S}_2) - \vec{F}\cdot\vec{j}_2 - \varepsilon_{th}\vec{F}\cdot\vec{\chi}_{n_2} = n_2 C_{w_2}. \tag{3}$$

where $n_2 = \int_{\varepsilon\geq\varepsilon_{th}} f(\vec{k})d^3k$, $\vec{j}_2 = n_2\vec{V}_2$, $\vec{V}_2 = \langle\vec{v}\rangle_{\varepsilon\geq\varepsilon_{th}}$, $\hat{U}_2 = \langle\vec{v}\hbar\vec{k}\rangle_{\varepsilon\geq\varepsilon_{th}}$, $\vec{S}_2 = \langle\vec{v}\varepsilon\rangle_{\varepsilon\geq\varepsilon_{th}}$, $\vec{\chi}_{n_2} = \frac{1}{\hbar}\oint_{\epsilon=\epsilon_{th}} f_{\vec{k}}d\vec{s}_k$, $\hat{\chi}_{p_2} = \frac{1}{\hbar}\oint_{\epsilon=\epsilon_{th}}\hbar\vec{k}f_{\vec{k}}d\vec{s}_k$, $C_{n_2} = \langle|\frac{\delta f}{\delta t}|_{coll}\rangle_{\varepsilon\geq\varepsilon_{th}}$, $\vec{C}_{p_2} = \langle\hbar\vec{k}|\frac{\delta f}{\delta t}|_{coll}\rangle_{\varepsilon\geq\varepsilon_{th}}$, and $\vec{F} = -q\vec{E}$.

The Monte Carlo (MC) data for inhomogeneous simulation indicate that the HES carrier velocity, $\vec{V}_2$, is fairly constant for the region where II is noticeable [2]. Since V_2 is nearly constant, we can bypass Eq.(2). The dependent variables are now reduced from n_2, $\vec{V}_2$, and w_2 to $\vec{j}_2$ and w_2. Also note that $\vec{S}_2$ can be approximated by $\vec{S}_2 \simeq \vec{V}_2 w_2$ as was described in [1]. Rewriting $n_2\vec{S}_2$ as $\vec{j}_2 w_2$ and expanding $\nabla\cdot(\vec{j}_2 w_2) = (\nabla\cdot\vec{j}_2)w_2 + (\vec{j}_2\cdot\nabla)w_2$, Eq.(1) and (3) can be combined to yield

$$\hat{a}\cdot\nabla w_2 - \vec{F}\cdot\hat{a}\,[1-(w_2-\varepsilon_{th})\gamma_{n_2}] = \frac{n_2}{|\vec{j}_2|}(C_{w_2} - w_2 C_{n_2}), \tag{4}$$

where $\hat{a} = \frac{\vec{j}_2}{|\vec{j}_2|}$ and $\gamma_{n_2} = \frac{\vec{\chi}_{n_2}\cdot\hat{a}}{|\vec{j}_2|}$.

If we further assume that γ_{n_2}, C_{w_2}, and C_{n_2} can be expressed as a function of w_2 and its spatial derivatives, i.e.,

$$(w_2-\varepsilon_{th})\gamma_{n_2} \approx g_0(w_2) + g_1(w_2)\hat{a}\cdot\nabla w_2, \tag{5}$$

$$\frac{n_2}{|\vec{j}_2|}(C_{w_2} - w_2 C_{n_2}) \approx -(w_2-\varepsilon_{th}) \cdot[k_0(w_2) + k_1(w_2)\hat{a}\cdot\nabla w_2], \tag{6}$$

we then obtain:

$$[1 + k_1(w_2)(w_2-\varepsilon_{th}) + \vec{F}\cdot\hat{a}g_1(w_2)]\,\hat{a}\cdot\nabla(w_2) + k_0(w_2)(w_2-\varepsilon_{th}) = \vec{F}\cdot\hat{a}\,[1-g_0(w_2)]. \tag{7}$$

In the 1-D case, Eq.(7) becomes

0-7803-3775-1/97/$10.00 © 1997 IEEE.

$$(1+\lambda_{w_2})\frac{dw_2}{dx}+k_0(w_2)(w_2-\varepsilon_{th})=F\left[1-g_0(w_2)\right] \quad (8)$$

where $\lambda_{w_2}=k_1(w_2)(w_2-\varepsilon_{th})+Fg_1(w_2)$ and $F=\mid \vec{F} \mid$.

The physical interpretation of Eq.(8) is very clear. The reciprocal of $k_0(w_2)$ represents the w_2-dependent mean-free-path length [3] for HES's and $[1-g_0(w_2)]$ represents a modification factor to F because there is particle(and hence also energy) exchange between the low- and high-energy electrons in the two-population HD model [1]. The parameter λ_{w_2} characterizes the deviation of the inhomogeneous MC data from that of the homogeneous one, depicting the highly non-local and non-equilibrium nature of the high-energy electron distribution.

The newly derived simplified HES HD equation, Eq.(8), is analogous to the energy transport equation of Cook and Frey [4], used by Agostinelli et al. [5]:

$$\frac{dw}{dx}+\frac{9}{20}\left[\frac{40}{9}\frac{m^*(w-w_0)}{\tau_p\tau_w}+F^2\right]^{\frac{1}{2}}=\frac{21}{20}F \quad (9)$$

where w is the average carrier energy of TEP, $w_0=0.039$ eV, m^* is the effective mass of the electron, τ_p is the momentum relaxation time, and τ_w is the energy relaxation time.

III. Model Parameters Extraction

An MC simulator is developed employing the band structure based on the isotropic two-band model by Jin et al. [6]. Using both bulk and device MC data, we can explicitly evaluate the term $\vec{F}\cdot\vec{\chi}_{n_2}$ appearing in Eq.(1), and consequently, γ_{n_2}. Similarly, both C_{n_2} and C_{w_2} can be evaluated from the MC simulation. Using the assumptions Eqs.(5) - (6), we can obtain a parameterized expressions for $g_0(w_2)$ and $k_0(w_2)$ respectively by best fitting to the homogeneous MC data (see Fig.1). Note that the parameterized expression for $g_0(w_2)$ and $k_0(w_2)$ are independent of device or bias. The data for $g_1(w_2)$ and $k_1(w_2)$, however, must be obtained from various device simulations under different bias conditions.

Instead of individually modeling $g_1(w_2)$ and $k_1(w_2)$, it is more convenient to model λ_{w_2} directly. Once we have decided to approximate the energy transport equation for w_2 to be of the form given by Eq.(8), we can directly determine λ_{w_2} by assuming as if Eq.(8) were an exactly balanced equation. The result of λ_{w_2} based on Eq.(8) from various n^+-n-n^+ diode simulations under different bias conditions is shown in Fig.2. Although these MC data are quite scattered but two distinct features emerge from these data. For the increasing w_2 (electron heating), λ_{w_2} is fairly constant ($\approx$ -0.3). For the decreasing w_2 (electron cooling), however, λ_{w_2} is distinctly different from that of the increasing w_2. As w_2 decreases, not only λ_{w_2} changes its sign but also it changes magnitude; it increases first and then decreases again. For simplicity, we choose a piece-wise constant model for λ_{w_2} :

$$\lambda_{w_2}=\begin{cases}-0.3 & \text{for } \frac{dw_2}{dx}>0\\ 0.3 & \text{for } \frac{dw_2}{dx}<0.\end{cases} \quad (10)$$

Now it remains to express the II coefficient α as a function of w_2. This is achieved by a simple formula involving an effective field expression fitted to our homogeneous MC simulation data:

$$\alpha(w_2)=\begin{cases}9.59\times10^5 e^{(\frac{-1.34\times10^2}{E_{eff}})} & \text{for } \Delta w_2>0.164\\ 1.156\times10^4 e^{\frac{(-0.9\times10^2}{E_{eff}})} & \text{otherwise,}\end{cases} \quad (11)$$

where $\Delta w_2=w_2-\varepsilon_{th}$, $\varepsilon_{th}=1.12eV$, α is in unit of $\frac{1}{cm}$, and $E_{eff}(w_2)=0.002+0.77\Delta w_2-0.80\Delta {w_2}^2+0.36\Delta {w_2}^3+0.14\Delta {w_2}^4$ is in unit of $\frac{MV}{cm}$. Note that this E_{eff} is different from the steady-state local electric field, E, applied to the electron under device operation. Instead, it represents an effective electric field and is a function of the average energy of HES obtained from solving the simplified HES HD model.

IV. Numerical Procedures and Results

Eq.(8) is first solved with $\frac{dw_2}{dx}$ set to zero. By solving the homogeneous balance equation $k_0(w_2)(w_2-\varepsilon_{th})=F\left[1-g_0(w_2)\right]$ for a small constant electric field (say $E_0=10.0kV/cm$) mimicking the low-field n^+- region on both source and drain sides, we can can obtain the boundary value $w_2(0)$ at $x=0$. We then replace the original electric field $E(x)$ with E_0 whenever $\mid E(x) \mid \leq E_0$. Since $F(x)$ is a known function of x, as an initial guess, we may use $w_2(F(x))$ which can be obtained from the homogeneous MC data. Eq.(7) is discretized using the upwind scheme. The calculated boundary value for w_2 is specified at $x=0$ (the source boundary) but left to be determined at $x=L$ (the drain boundary).

Fig.3 shows comparison of w_2 between the HES HD and the MC model for two different 1-D n^+-n-n^+ structures and different bias conditions. The agreement is not perfect but quite acceptable. For comparison purpose, we have also implemented the TEP HD model used by [5] which is based on Eq.(9). Their model uses transport parameters, τ_p, and τ_w based on the homogeneous MC data [7]. Since the MC data used in this work and the one used in [7] are not the same, we provide two versions of the TEP model. One is the model with transport

parameters based on this work, i.e., UMass TEP (UM-TEP) HD model, and the other using original UTexas group's transport parameters - UTexas TEP (UT-TEP) HD model [7]. Since E_{eff} is a measure of non-local effect and the primary parameter directly affecting α, in Fig.4, we compare E_{eff} for three different models: HES HD, UM-TEP HD and UT-TEP HD. All three HD models show distinctive non-local behavior of electrons as indicated by the effective field profiles. Before the local electric field E reaches its peak E_{max}, the effective field E_{eff} always remains smaller than E. This spatial delay between E_{eff} and E is known as the "dead space" [8]. However, after passing the E_{max}, E_{eff} still remains non-zero in the region where almost all the electrons return to the thermal equilibrium. Note that E_{eff} based on the HES HD model shows a longer spatial relaxation distance than those based on both TEP HD models. This relaxation distance directly affect the shape of α and is sensitive to the choice of the parameter λ_{w_2} for $\frac{dw_2}{dx} < 0$.

Fig.5 finally compares α for three models with the MC data as a reference. The HES HD model and MC shows very good agreement for α over eight orders of magnitude difference, whereas, the α based on both TEP models, UM-TEP and UT-TEP, drops rather rapidly after passing the maximum α for both $n^+ - n - n^+$ devices. This is due to a smaller relaxation distance of the two TEP HD models compared to that of the HES HD model. Also notice that the α based on the UT-TEP model underestimates its peak value more than other models.

V. Discussion

The HES HD transport equation, Eq.(7), represents a simplification/approximation to the system of three HES transport equations Eqs.(1) - (3). The momentum transport equation, Eq.(2), is totally bypassed because $\vec{V_2}$, which appears in the modeling of $k_0(w_2)$ and $k_1(w_2)$, turns out to be fairly constant in the region of appreciable II. The remaining two transport equations are combined into one resulting in a single first-order transport equation for w_2. The only MC calibrated transport parameters are $k_0(w_2)$ and $g_0(w_2)$ from the bulk simulation data and $\lambda(w_2)$ from the device simulation data. By choosing a simple piece-wise constant for $\lambda(w_2)$, we have obtained a fairly good agreement with the MC results. In order to apply the HES HD model to 2-D or higher dimensions, however, we must assume the direction of the conventional current flow($\vec{j}$) and that of HES current flow($\vec{j_2}$) to be parallel to each other. We believe this to be a reasonable assumption.

The advantage of solving only one transport equation for w_2 is obvious. It is robust and computationally very efficient. By solving the 1-D HES energy transport equation along each of many current flow lines, a 2-D distribution of α can be easily obtained by using the effective field concept. The only input to the HES HD solver is the electric field profile readily obtainable from the conventional DD or HD solver. To demonstrate the applicability of this new HD model to 2-D problems, α obtained by solving n-channel LDD MOSFET is shown in Fig.6.

References

[1] P. G. Scrobohaci and T.-w. Tang, "Modeling of the hot electron subpopulation and its application to impact ionization in submicron silicon devices - part I: transport equation," *IEEE Transactions on Electron Devices*, vol. 41, no. 7, p. 1197, 1994.

[2] C.-S. Yao, J.-G. Ahn, Y.-J. Park, H.-S. Min, and R. W. Dutton, "Formulation of a tail electron hydrodynamic model based on Monte Carlo results," *IEEE Electron Device Letters*, vol. 16, no. 1, p. 26, 1995.

[3] J. Slotboom, G. Streutker, M. Dort, P. Woerlee, A. Prujijmboom, and D. Gravesteijn, "Non-local impact ionization in silicon devices," *IEDM*, p. 127, 1991.

[4] R.K.Cook and J.Frey, "Two-dimensional simulation of energy transport effects in Si and GaAs MESFETs," *IEEE Transactions on Electron Devices*, vol. 29, p. 970, 1982.

[5] V. Agostinelli, T. Bordelon, X. Wang, K.Hasnat, C. Yeap, D.B.Lemersal, A. Tasch, and C. Maziar, "Two-dimensional energy dependent models for the simulation of substrate current in submicron MOSFET's," *IEEE Transactions on Electron Devices*, vol. 41, no. 10, p. 1784, 1994.

[6] G. Jin, R. W. Dutton, Y.-J. Park, and H.-S. Min, "An isotropic two band model for hot electron transport in silicon: including electron emission probability into SiO_2," *Journal of Applied Physics*, vol. 78, no. 5, p. 3174, 1995.

[7] K. Hasnat, C. F. Yeap, J. Jallepalli, W. K. Shih, A. Hareland, V. M. Agostinelli, A. F. Tasch, and C. Maziar, "A pseudo-lucky electron model for simulation of electron gate current in submicron NMOSFET's," *IEEE Transactions on Electron Devices*, vol. 43, no. 8, p. 1264, 1996.

[8] S. A. Plimmer, J. P. R. David, D. C. Herber, T. W. Lee, G. J. Rees, P. A. Houston, R. Grey, P. N. Robson, A. W. Higgs, and D. R. Wight, "Investigation of Impact Ionization in Thin GaAs Diodes," *IEEE Transactions on Electron Devices*, vol. 43, no. 7, p. 1066, 1996.

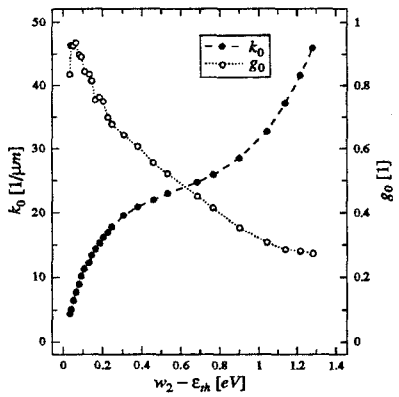

Figure 1: Plot of $k_0(w_2)$ and $g_0(w_2)$ versus $w_2 - \varepsilon_{th}$.

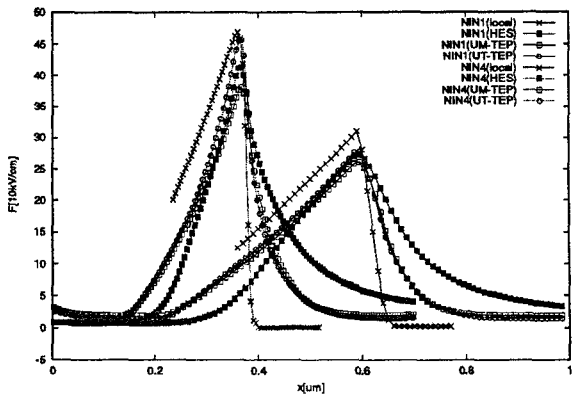

Figure 4: Comparison of E_{eff} for the local field, the effective field based on the HES, UM-TEP, and UT-TEP HD models.

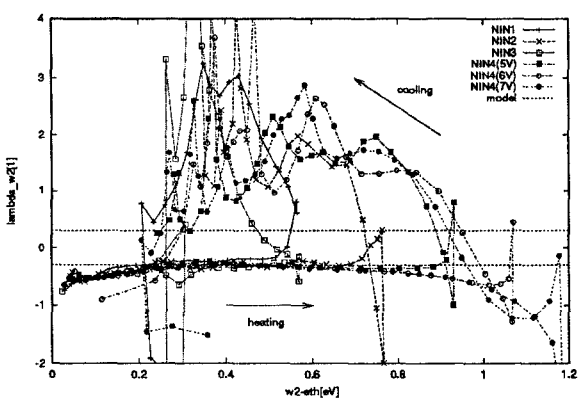

Figure 2: Plot of λ_{w_2} versus $w_2 - \varepsilon_{th}$.

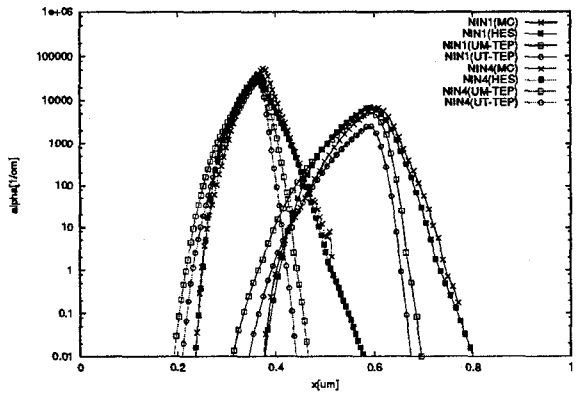

Figure 5: Comparison of α obtained from the MC, HES, UM-TEP, and UT-TEP HD models.

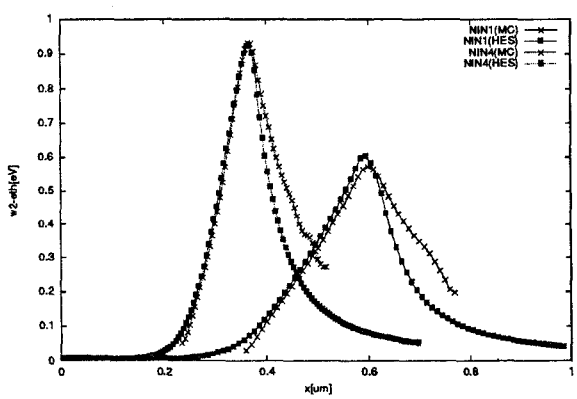

Figure 3: Comparison of w_2 obtained from the MC and the simplified HES-HD model.

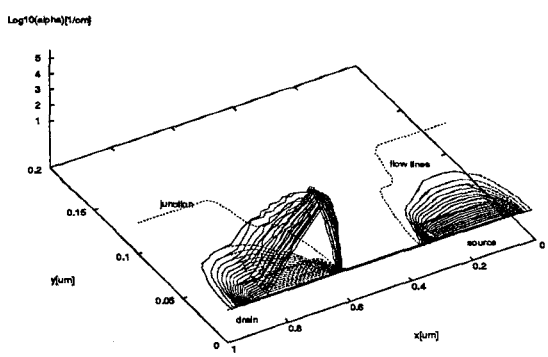

Figure 6: A 2-D distribution of α along the current flow lines for 0.25 μm n-channel LDD MOSFET at V_g=3V and V_d=5V.